

Gelatin Effects on the Physicochemical and Hemocompatible Properties of Gelatin/PAAm/Laponite Nanocomposite Hydrogels

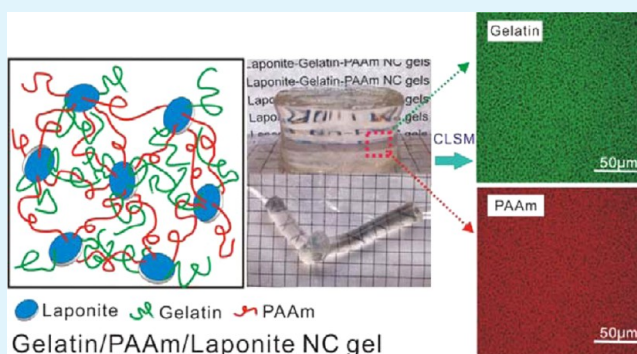
Changpeng Li,[†] Changdao Mu,[†] Wei Lin,^{*,‡} and To Ngai^{*,§}

[†]Department of Pharmaceutical and Bioengineering, School of Chemical Engineering, and [‡]Department of Biomass and Leather Engineering, Key Laboratory of Leather Chemistry and Engineering of Ministry of Education, Sichuan University, Chengdu 610065, P. R. China

[§]Department of Chemistry, The Chinese University of Hong Kong, Shatin, N. T. Hong Kong

ABSTRACT: In recent years, inorganic nanoparticles such as Laponite have frequently been incorporated into polymer matrixes to obtain nanocomposite hydrogels with hierarchical structures, ultrastrong tensilities, and high transparencies. Despite their unique physical and chemical properties, only a few reports have evaluated Laponite-based nanocomposite hydrogels for biomedical applications. This article presents the synthesis and characterization of a novel, hemocompatible nanocomposite hydrogels by in situ polymerization of acrylamide (AAm) in a mixed suspension containing Laponite and gelatin. The compatibility, structure, thermal stability, and mechanical properties of the resulting NC gels with varied gel compositions were investigated. Our results show that the prepared nanocomposite hydrogels exhibit good thermal stability and mechanical properties. The introduction of a biocompatible polymer, gelatin, into the polymer matrix did not change the transparency and homogeneity of the resulting nanocomposite hydrogels, but it significantly decreased the hydrogel's pH-responsive properties. More importantly, gelatins that were incorporated into the PAAm network resisted nonspecific protein adsorption, improved the degree of hemolysis, and eventually prolonged the clotting time, indicating that the in vitro hemocompatibility of the resulting nanocomposite hydrogels had been substantially enhanced. Therefore, these nanocomposite hydrogels provide opportunities for potential use in various biomedical applications.

KEYWORDS: Laponite, PAAm, gelatin, hemocompatible, nanocomposite hydrogels



Despite the unique physical and chemical properties, only a few reports have evaluated nanoclay-based NC hydrogels for biorelated applications. This might be due to the fact that NC hydrogels generally require a further modification to improve their biocompatibility to satisfy biomedical applications such as controlled cell adhesion surfaces, injectable drug delivery matrixes, and antimicrobial films.^{4–6} Indeed, Haraguchi et al. prepared a poly(*N*-isopropylacrylamide) (PNIPAM)/Laponite NC hydrogel and explored its feasibility for cell cultivation and cell sheet detachment.⁷ It was found that the addition of Laponite could enhance the cell adhesion characteristics when compared with those of pure PNIPAM hydrogels. However, the negatively charged surface of the Laponite could adsorb proteins, which could, in turn, initiate thrombosis by activation of factor XII.⁸ Therefore, in biomedical applications, a further modification is required to balance the cell adhesion characteristics and the antithrombogenicity of the prepared NC hydrogels.

INTRODUCTION

Hydrogels, which contain three-dimensional polymeric networks and have remarkable capacities to hold water, have attracted great attention because of their potential applications in technological and biomedical fields. However, because of the restricted molecular motion of the polymer chains caused by the large amount of cross-links arranged randomly, most prepared hydrogels are soft, weak, and brittle, which greatly limits their practical applications.¹ In recent years, considerable effort has been made to overcome this problem, and one important breakthrough was the creation of nanocomposite (NC) hydrogels, first produced by Haraguchi et al. in 2002.² NC gels are hydrogels synthesized by incorporating clay nanoparticles in the polymer matrix. They often are prepared by in situ free-radical polymerization at high yield under mild conditions (near ambient temperature, without stirring), in which clay nanoparticles act as multifunctional cross-linkers and polymer chains are attached to their surfaces through ionic or polar interactions, resulting in the formation of unique organic/inorganic networks. The resulting NC hydrogels are thus tough and transparent and have excellent thermal and mechanical properties.³

Despite the unique physical and chemical properties, only a few reports have evaluated nanoclay-based NC hydrogels for biorelated applications. This might be due to the fact that NC hydrogels generally require a further modification to improve their biocompatibility to satisfy biomedical applications such as controlled cell adhesion surfaces, injectable drug delivery matrixes, and antimicrobial films.^{4–6} Indeed, Haraguchi et al. prepared a poly(*N*-isopropylacrylamide) (PNIPAM)/Laponite NC hydrogel and explored its feasibility for cell cultivation and cell sheet detachment.⁷ It was found that the addition of Laponite could enhance the cell adhesion characteristics when compared with those of pure PNIPAM hydrogels. However, the negatively charged surface of the Laponite could adsorb proteins, which could, in turn, initiate thrombosis by activation of factor XII.⁸ Therefore, in biomedical applications, a further modification is required to balance the cell adhesion characteristics and the antithrombogenicity of the prepared NC hydrogels.

Received: June 14, 2015

Accepted: July 23, 2015

Published: July 23, 2015

An efficient strategy for improving the hemocompatibility of biomaterials and reducing protein adsorption is the modification of the surface of the biomaterials with hydrophilic polymers such as poly(ethylene glycol) (PEG) or antithrombotic agents. It is assumed that PEG coatings can resist platelet adhesion and protein adsorption through steric repulsion due to polymer chain compression.^{9,10} However, the effectiveness of such surface modification in preventing thrombogenicity is still a matter of debate.¹¹ Heparin has also been used to modify the surfaces of biomaterials, and its application has reached the commercial stage in some cardiovascular devices.¹² However, the in vivo biocompatibility of the heparin coating has not been evaluated in detail.^{13,14}

Gelatin is a polypeptide that can be obtained by the hydrolytic degradation of collagen. Because of its excellent biocompatibility, biodegradation, and hydrophilicity, gelatin has been widely used in various medical applications such as scaffold materials,^{15–17} wound dressings,^{18–20} and drug delivery devices.^{21,22} Moreover, it has been employed as a plasma expander and blood substitute since the 1940s.^{23,24} Recently, Manju et al. fabricated a gelatin-based hydrogel to modify a polyester vascular graft. They showed that a hydrogel containing a gelatin coating can effectively prevent the adhesion of platelets and leukocytes, thus offering a biocompatible and low-thrombogenic surface.²⁵ Bundela and Bajpai successfully produced a hydroxyapatite–gelatin-based porous matrix as a bone substitute and found that increasing the amount of gelatin can greatly decrease the weight of blood clots and the extent of bovine serum albumin (BSA) adsorption.²⁶ Therefore, gelatin can be treated as a hydrophilic polymer that not only provokes no damage to blood cells or activation of plasma proteins but also improves the smoothness of the surfaces, resulting in better antithrombogenicity properties of biomaterials.

In this article, a novel hemocompatible protein/polymer–clay NC hydrogel was successfully synthesized through the in situ polymerization of acrylamide (AAM) in a mixed suspension of Laponite and gelatin. The compatibility, morphology, and mechanical properties of the resulting bioactive NC hydrogels with varying gel compositions were investigated. Confocal microscopy was used to investigate how the labeled gelatin chains were distributed in the gel network. Moreover, the effects of introducing gelatin on the stimuli-responsive swelling behavior and the physicochemical and biological properties of the resulting protein/polymer–clay NC hydrogels were evaluated for required applications.

EXPERIMENTAL SECTION

Materials. Acrylamide (AAM), gelatin (type B, BC; ~250 Bloom, $M_w \approx 100$ kDa), and bovine serum albumin (BSA) were purchased from Aladdin Inc. The synthetic hectorite Laponite RDS $\{Na^{+}_{0.7}[(Si_8Mg_{0.5}Li_{0.3})O_{20}(OH)_4]^{-0.7}\}$, modified with pyrophosphate ions, was kindly provided by Rockwood. N,N' -Methylenebis(acrylamide) (BIS), ammonium persulfate (APS), and N,N,N',N' -tetramethylethylenediamine (TEMED) were purchased from Sigma-Aldrich and used without further purification. The fluorescent dyes methacryloxyethyl thiocarbonyl rhodamine B (MRB) and fluorescein isothiocyanate (FITC) were purchased from Polysciences Inc. A stock suspension of Laponite RDS at 5% w/v was prepared with deionized water under stirring for at least 6 h. The concentrations of the stock solutions of TEMED (liquid), APS, and BIS were fixed at 10% v/v, 4% w/v and 0.8% w/v, respectively. They were freshly prepared just before use.

Synthesis of Gelatin/PAAm/Laponite Nanocomposite Hydrogels. The hydrogels were synthesized through the in situ radical polymerization of the monomer (AAM) in an aqueous suspension of

Laponite RDS and gelatin with a small amount of BIS as a co-cross-linker. The molar ratio between AAM, the accelerator (TEMED), the initiator (APS), and BIS was 100:0.735:0.426:0.05, and the initial concentration of AAM was kept at 10% w/v, whereas the concentrations of Laponite and gelatin were varied between 0 and 2% w/v. The concentrations of TEMED, APS, and BIS were then 0.06% v/v, 0.08% w/v, and 0.01% w/v, respectively. First, the gelatin solution (5% w/v) was dissolved in water and heated at 40 °C for 1 h. A Laponite suspension (0–4 mL), BIS (140 μ L), and AAM (1.0 g) were added into a 15 mL glass tube, and then gelatin (0–4 mL) was introduced. The total volume of the solution mixture was fixed at 9.74 mL with deionized water. After being immersed in a water bath at 50 °C for 2 h, the mixture became a transparent solution. Nitrogen gas was bubbled through the solution for 10 min, and then APS (200 μ L) and TEMED (60 μ L) were added. The radical polymerization was carried out in a water bath at 25 °C for 24 h. After polymerization, the hydrogels were removed from the tubes and separated into two parts. Some of the samples were stored in the as-prepared state for swelling and mechanical properties tests, and the rest were soaked in deionized water for 3 days with the water changed every 8 h to remove residual unreacted monomers.

In this article, the prepared gelatin/PAAm/Laponite nanocomposite hydrogels are denoted as $LxGy$, where L and G indicate Laponite RDS and gelatin, respectively, and x and y represent the corresponding concentrations in the form $100 \times$ Laponite/water (w/v) and $100 \times$ gelatin/water (w/v), respectively. For example, L2G2 represents a gel containing Laponite with a Laponite/water ratio of 2% w/v and gelatin with a gelatin/water ratio of 2% w/v.

Synthesis of the Fluorescent Gelatin/PAAm/Laponite Nanocomposite Hydrogels. The fluorescent gelatin/PAAm/Laponite nanocomposite hydrogels consisted of FITC-labeled gelatin, MRB-labeled PAAm, and the nanoclay Laponite. The labeling was based on the method reported by Schreiber and Haimovich.²⁷ Typically, 100 mL of the 5% w/v aqueous gelatin solution was adjusted to pH 8.5 with sodium hydroxide (NaOH) solution. FITC was dissolved in water at a concentration of 0.01 mg/mL, also with a pH of 8.5. Then, 100 mL of FITC solution was added to the gelatin solution, and the mixture was stirred for 8 h at 40 °C. Free FITC was removed by ethanol extraction, and then the FITC-labeled gelatin was dried in an oven at 50 °C. The method for synthesizing the fluorescent hydrogels was the same as that described for FITC-labeled gelatin instead of normal gelatin, and 100 μ L of MRB solution (0.1 mg/mL) was added to the mixture before the bubbling of nitrogen gas.

Fourier Transform Infrared (FTIR) Spectroscopy. The samples were freeze-dried in a lyophilizer (Christ ALPHA 1–2 LD) for 24 h at –50 °C. Infrared spectra were recorded for samples as KBr pellets with an FTIR spectrophotometer in the range of 800–4000 cm^{-1} .

Scanning Electron Microscopy (SEM). For SEM observations, the samples were freeze-dried in a lyophilizer (Christ ALPHA 1–2 LD) for 24 h at –50 °C and then coated with Au before imaging on an FEI Quanta 400FEG microscope operating at 20 kV.

Confocal Laser Scanning Microscopy (CLSM). Confocal microscopy images of the NC hydrogels were recorded on a Nikon Eclipse Ti inverted microscope (Nikon, Tokyo, Japan). Lasers with wavelengths of 543 and 488 nm were used to excite the fluorescent NC hydrogels.

Measurements of Thermal Properties. Measurements of thermal properties were carried out on a thermogravimetric analyzer (NETZSCH TG 209F1, Selb, Germany) from 40 to 750 °C at a heating rate of 10 °C/min under a nitrogen atmosphere. All samples were freeze-dried, and the total mass of each sample was 3 mg.

Measurements of Mechanical Properties. Compressive and tensile tests were performed on the as-prepared NC gel samples with an MTS Universal Testing Machine (CMT6202, MTS Systems Co., Ltd., Shanghai, China) at room temperature. In the compressive tests, cylindrical NC gel samples of 20-mm diameter and 10-mm thickness were set on the lower plate and compressed by the upper plate with a deformation rate at 5 mm/min until the compressive strain reached 90%. The compressive stress (σ) was calculated as

$$\sigma = F/\pi r^2 \quad (1)$$

where F and r are the force loaded on the hydrogel and the initial unload radius, respectively.

In the tensile tests, the conditions were as follows: sample size, 4.5-mm diameter and 50-mm length; gauge length between the jaws, 30 mm; and crosshead speed, 100 mm/min. The tensile stress (σ^*) was calculated with the equation

$$\sigma^* = \frac{F}{A} = \frac{FL}{A_0 L_0} \quad (2)$$

where F , A , A_0 , L , and L_0 are the force applied on the hydrogel, the real-time cross-sectional area of the deformed hydrogel, the initial cross-sectional area of the hydrogel, the real-time gauge length of the deformed hydrogel and the initial gauge length of the hydrogel, respectively. The largest tensile stress and strain are defined as the tensile strength at break (σ_b) and the elongation ratio at break (ϵ_b), respectively. The Young's modulus (E) in the range of 10% strain was calculated from the slope of the stress–strain curve. At least three samples were used for each test.

Swelling Experiments. Swelling experiments were performed at room temperature by immersing the as-prepared hydrogels in pure water and also in buffer solutions to reach swelling equilibrium. After that, the swollen gels were dried. The effects of pH and ionic strength on the equilibrium swelling ratio (ESR) were investigated. The pH was varied from 3 to 12 at a constant ionic strength of $I = 0.01$ M. The ionic strength was changed from 0 to 0.1 M at room temperature. The equilibrium swelling ratio was calculated as

$$\text{ESR} = \frac{W_s - W_d}{W_d} \quad (3)$$

where W_s is the weight of the swollen gel and W_d is the weight of the dry gel.

In Vitro Blood Compatibility. *Bovine Serum Albumin (BSA) Adsorption.* The adsorption of BSA onto the surfaces of the hydrogels was performed by the batch contact method to investigate the interaction between blood protein and the hydrogel surfaces.²⁸ In a typical experiment, a BSA solution (0.2% w/v) was prepared in 0.5 M phosphate-buffered saline (PBS) at pH 7.4. A piece of hydrogel was first immersed in a test tube containing PBS to swell for 72 h and then weighed, after which 20 mL of BSA solution was added. After the tube had been shaken gently at 37 °C for 30 min, the concentration of residual BSA was determined in terms of the absorbance of the supernatant at 277 nm by UV–vis spectrometer (Perkin-Elmer Lambda 25). The amount of protein adsorbed was calculated according to the equation

$$\text{adsorbed BSA} = \frac{C_0 - C_a}{W} V \quad (4)$$

where C_0 and C_a denote the BSA concentrations (mg/mL) before and after adsorption, respectively; W is the weight of the swollen hydrogel piece (g); and V is the volume of the BSA solution (mL).

Blood Dynamic Clotting Test. The anticoagulant properties of gelatin/PAAm/Laponite nanocomposite hydrogels were evaluated by the kinetic clotting time method.^{29,30} Typically, 4.0 mL of whole blood obtained from a healthy rabbit was anticoagulated by addition of 1.0 mL of anticoagulant citrate dextrose (ACD) solution and then diluted with 5.0 mL of 0.9% saline. The hydrogels were equilibrated with 0.9% saline for 72 h and sterilized with UV light for 5 min. Then, 200 μ L of diluted ACD blood was dropped on the surfaces of the samples and glass coverslips, after which 25 μ L of CaCl_2 (0.2 mol/L) solution was added and mixed uniformly. After a predetermined period of time (5, 10, 20, 30, 40, and 50 min), the samples were placed into 100 mL of deionized water and incubated at 37 °C for 10 min. The red blood cells that had not trapped in the thrombus were hemolyzed, and the free hemoglobin was dispersed in the water. The concentration of free hemoglobin in water was measured in terms of the absorbance of the supernatant at 545 nm by UV–vis spectrometer. A solution of 200 μ L

of diluted ACD blood in 100 mL of water was used as the control. The blood-clotting index (BCI) was calculated as

$$\text{BCI} (\%) = \frac{\text{OD}_t}{\text{OD}_c} \times 100 \quad (5)$$

where OD_t and OD_c denote the OD values of the test and control samples, respectively.

Hemolysis Assay. The hemolytic potential of a material is a measure of the extent of hemolysis that can be caused by the material when it comes into contact with blood.³¹ The hemolytic potential of the gelatin/PAAm/Laponite nanocomposite hydrogels was investigated according to the reported procedure.²⁹ The hydrogels were placed in a test tube with 10 mL of 0.9% saline and incubated for 30 min at 37 °C; then, 200 μ L of diluted ACD blood was added to the test tube, and the mixture was incubated for 60 min at 37 °C. A separate sample of 100% hemolysis induced by 10 mL of deionized water was used as a positive control, and 0% hemolysis in 0.9% saline without added hydrogel was used as a negative control. After the incubation, all of the samples were centrifuged at 2000 rpm for 5 min, and the optical density (OD) of the supernatant was determined for the absorbance at 545 nm by a UV–vis spectrometer. The percentage hemolysis was calculated as

$$\text{hemolysis} (\%) = \frac{(\text{OD}_t - \text{OD}_n)}{\text{OD}_p - \text{OD}_n} \times 100 \quad (6)$$

where OD_t , OD_n , and OD_p denote the OD values of the test, negative, and positive samples, respectively. The reported hemolysis results are averages of six measurements.

RESULTS AND DISCUSSION

Preparation and Structural Characterization of the NC Gels. Figure 1 shows the proposed mechanism for the synthesis of nanocomposite hydrogels containing PAAm, Laponite, and gelatin. In the first step, gelatin solution was added to a dispersion of Laponite, AAm, and BIS. It can be seen that, within a few minutes, the solution turned from transparent into an opaque gel-like mixture (Figure 1a). This can be attributed to the fact that the surfaces of the Laponite RDS particles are negatively charged and the gelatin has strong polyampholytic properties so that it can be easily polarized by a charged surface. Such polarization could induce an attractive electrostatic interaction between the gelatin and the Laponite. In addition, the mixture of nanoclay and gelatin is in a semistable state, and the strong interaction between them can lead to a spinodal decomposition, resulting in a less transparent solution.³²

However, in the second step, when the mixture was immersed in a water bath at 50 °C for 2 h, the turbidity of the mixture decreased sharply (Figure 1b). Indeed, the mixture dispersion was able to maintain its transparency and liquid-like state for more than 1 day with the addition of AAm and BIS. This likely was caused by a reduction of the noncovalent interactions between the nanoclay and gelatin and the subsequent prevention of precipitation of the mixture when heated at 50 °C. Also, at higher temperature, gelatin chains might distribute more homogeneously and in an extended conformation in the mixture. Moreover, AAm and BIS can help to stabilize the dispersion by being adsorbed around the nanoclay, further weakening the electrostatic interactions between the nanoclays and gelatins.^{33,34}

In the third step, after bubbling of nitrogen for 10 min, APS and TEMED were gradually introduced into the mixture to initiate the polymerization. It is believed that the PAAm chains are grown from the surfaces of the clay platelets because of the higher concentration of APS and monomers around the clay

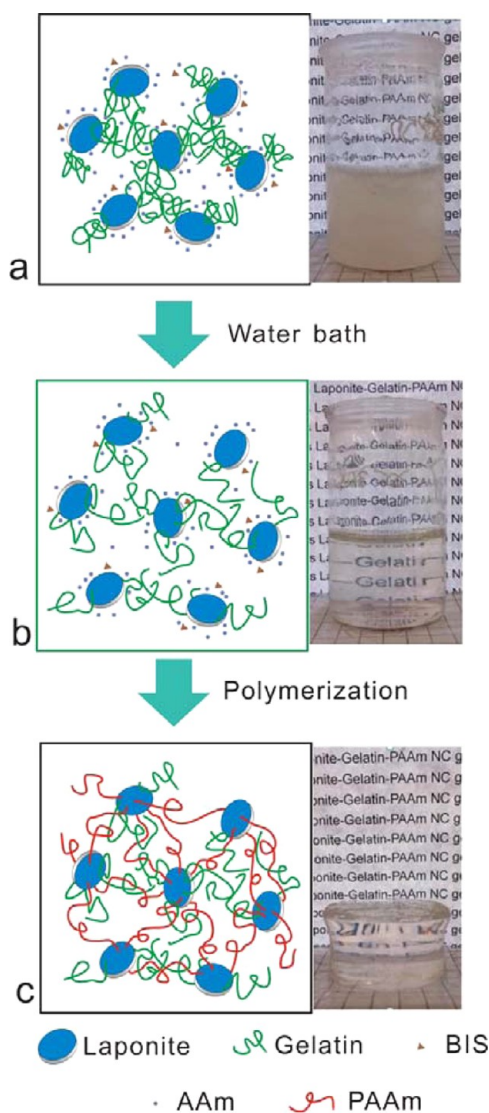


Figure 1. Three-step process involved in the synthesis of gelatin/PAAm/Laponite NC hydrogels. (a) Mixing gelatin with Laponite led to an opaque gel-like mixture. (b) Heating gelatin/Laponite at 50 °C resulted in a stable transparent dispersion. (c) Nanocomposite hydrogel structure formed after the polymerization of AAm and BIS.

platelets and that the polymer chains are attached to the surface of the clays nearby to form an NC gel (Figure 1c). The obtained NC gels can be easily shaped into fibers, sheets, or cylinders by using different forms of vessels. Note that the gelatin did not take part in the free-radical polymerization, but it could be interpenetrated into the PAAm/Laponite polymer matrix. In other words, the gelatin chains were immobilized inside the hydrogel network via through physical entanglements between the PAAm chains and interactions with the Laponite surface.

Figure 2 shows the FTIR spectra of hydrogels prepared by adding different contents of Laponite and gelatin. The two characteristic peaks at 1665 and 2927 cm^{-1} can be contributed to C=O stretching in the carboxamide functional group and C—H stretching, respectively. The intense peak at 1001 cm^{-1} is related to Si—O stretching in the nanoclay, and the adsorption band around 3427 cm^{-1} can be contributed to —NH stretching in the amide group and —OH stretching in Laponite. Additionally, there was no appearance of new

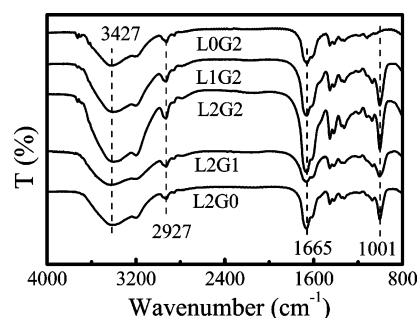


Figure 2. FTIR spectra of gelatin/PAAm/Laponite NC gels including samples L0G2, L1G2, L2G2, L2G1, and L2G0, synthesized with different amounts of Laponite and different gelatin concentrations.

vibrations, indicating that no new covalent bonds formed between the clay and the polymers in the nanocomposites after the addition of gelatin.

Lyophilization is known to preserve the structure and volume of the hydrogels even after all of the solvent has been removed.³⁵ Figure 3 shows typical SEM micrographs of the internal structures of the NC gels after the introduction of different amounts of gelatin. It can be seen that, after drying and the removal of frozen water, the resultant hydrogels were porous materials with tunable pore sizes, ranging from ~ 20 to $\sim 200 \mu\text{m}$. From Figure 3a–c, it was found that the presence of gelatin increased the pore size of the hydrogel from ~ 20 to $\sim 60 \mu\text{m}$. This is due to the significant hydrophilic character of the —NH₂ and —COO[−] groups linked to the primary gelatin chain. Such hydrophilic groups can increase the water uptake and network expansion, which further increases the voids in the hydrogel.^{36,37} However, the influence on the voids and, ultimately, the pore size induced by the gelatin content is not as substantial as that induced by Laponite. Figure 3c–e show that decreasing the Laponite content can significantly increase the pore size of the hydrogel because Laponite platelets can act as multifunctional cross-linkers. The lower the Laponite content, the larger the pore size in the hydrogel.³⁸

To see how gelatin chains are incorporated among the hydrogel networks, we first labeled gelatin with FITC through the reaction of the amino groups of gelatin with the isothiocyanate groups of FITC at pH 8.5. In addition, we copolymerized a fluorescent rhodamine monomer, MRB, with the monomer AAm so that the resultant PAAm polymer was also labeled. It is expected that FITC-labeled gelatin and MRB-labeled PAAm can be represented by a green channel (excitation wavelength of 488 nm) and red channel (excitation wavelength of 543 nm), respectively. It can be seen from Figure 4 that the distributions of gelatin and PAAm were homogeneous in the hydrogels,³⁹ indicating that the addition of gelatin did not lead to aggregation or induce any inhomogeneous phases in the hydrogel network. As a natural polyelectrolyte, gelatin can be readily adsorbed onto the negatively charged surface of Laponite by the induced interactions between the polyelectrolyte and the Laponite, as shown in Figure 1a.³² The CLSM results reveal that heating treatment of the initial mixtures before polymerization can make the gelatin distribute homogeneously in the resulting gel network. The deformation of the network structure has also been viewed when the hydrogel was under a tensile stress (Figure 4c,d). However, when the tensile force was released, the network recovered the original state, indicating the ability

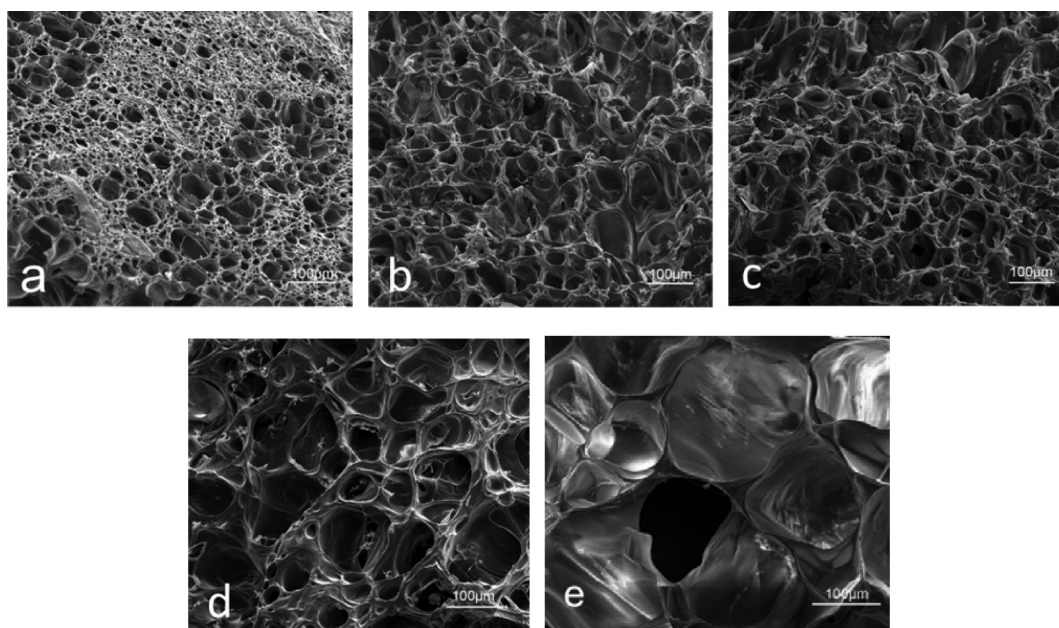


Figure 3. SEM micrographs of the prepared gelatin/PAAm/Laponite NC hydrogels including samples (a) L2G0, (b) L2G1, (c) L2G2, (d) L1G2, and (e) L0G2. The pore sizes of the NC gels range from ~ 20 to ~ 200 μm and increase with increasing gelatin content and decreasing Laponite content.

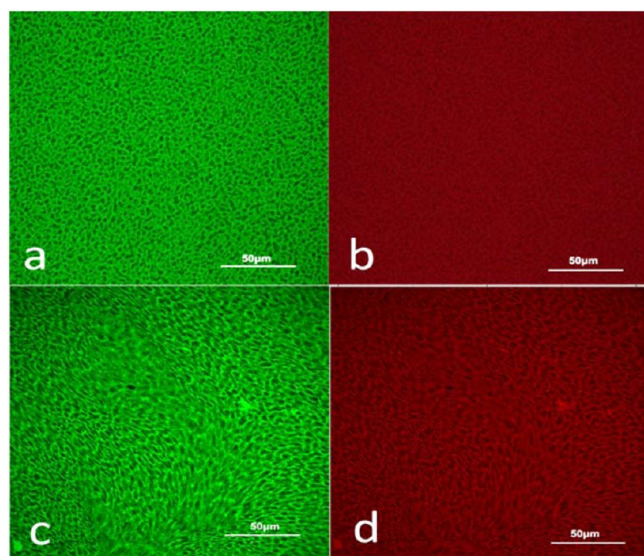


Figure 4. (a,b) CLSM images of L2G2 hydrogel excited at (a) 488 and (b) 543 nm. (c,d) Real-time CLSM observations of NC hydrogel excited at (c) 488 and (d) 543 nm under a tensile stress. The green images show the distribution of FITC-labeled gelatin, whereas the red images show the distribution of MRB-labeled PAAm inside the gel network.

to reversibly recover the resulting gelatin/PAAm/Laponite NC gels.

Thermal Properties of the NC Gels. Figure 5 shows the thermal properties of the synthesized NC hydrogels as measured by thermogravimetric analysis (TGA) and differential scanning calorimetry (DSC). It can be seen that the decomposition of the gelatin backbone started at 232 $^{\circ}\text{C}$ and extended to about 500 $^{\circ}\text{C}$, with a maximum decomposition rate at 323 $^{\circ}\text{C}$. In contrast, for all prepared NC gels, there were three decomposition stages, ranging from 40 to 750 $^{\circ}\text{C}$. The

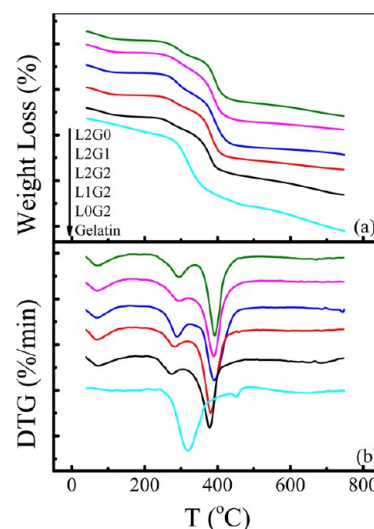


Figure 5. Measured (a) TGA and (b) DTG curves of the synthesized NC gels and the gelatin. Note that the thermal stability of the hydrogels is dependent on the content of Laponite.

first stage occurred between 40 and 200 $^{\circ}\text{C}$ and was due to the removal of bound water.

The second degradation stage (stage II), mainly due to loss of ammonia with formation of imide groups through cyclization, started from 200 to 300 $^{\circ}\text{C}$.⁴⁰ The third decomposition stage (stage III) for the NC gels, mainly corresponding to the decomposition of the polymer chains, occurred at 320 $^{\circ}\text{C}$ and extended to ~ 500 $^{\circ}\text{C}$. The thermal stability of the NC gel samples was calculated from their maximum temperatures in stages II and III and the initial temperature of stage III (Table 1). The results suggest that the thermal stability of the hydrogels was mainly determined by the content of Laponite. This is understandable because Laponite acts as a multifunctional cross-linker in NC gels and can effectively enhance the cross-link density of the hydrogel

Table 1. Maximum Temperatures of Stage II and Stage III and Initial Temperature of Stage III for Hydrogel Samples

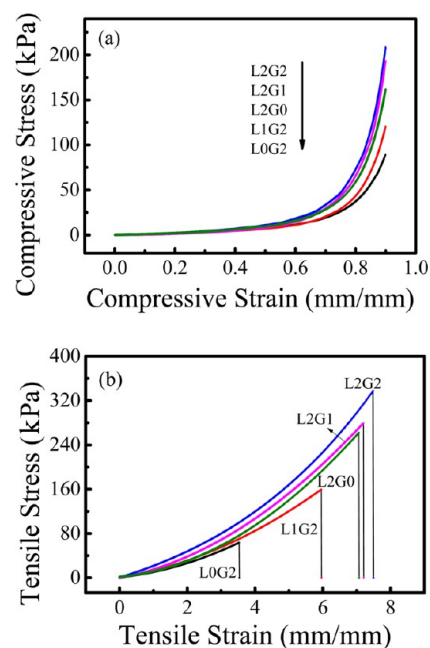
sample	maximum temperature (°C)		initial temperature of stage III (°C)
	stage II	stage III	
L2G0	295	393	330
L2G1	291	391	322
L2G2	293	390	320
L1G2	283	382	318
L0G2	274	377	302

network. The NC gels containing high contents of Laponite still retained good thermal stability even after the addition of gelatin. This could be related to the entanglements and hydrogen bonds among gelatin chains and the PAAm network, as well as the strong electrostatic interactions between Laponite and gelatin.^{41,42}

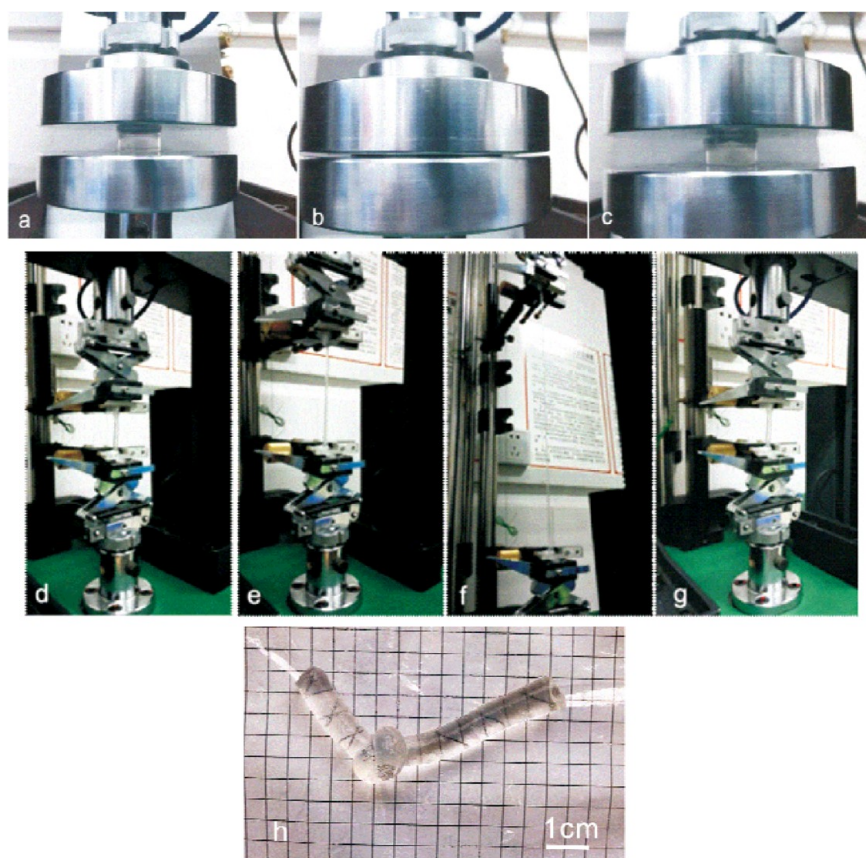
Tensile and Compressive Properties of the NC Gels.

Figure 6 shows the extraordinary mechanical toughness of the NC gels. All NC gel samples can sustained compression (Figure 6a–c), elongation (Figure 6d–g), and knotting (Figure 6h). Moreover, they had the ability to fully recover to the initial state when the load was released. The knotting behavior for the prepared NC gels revealed that they were highly elastic and stretchable.

The compressive stress–strain curves of the prepared NC gels are shown in Figure 7a. It can be seen that the samples could be compressed to a strain of 90%, and the stress at this strain was used to evaluate the mechanical strength of the NC

**Figure 7.** (a) Compressive stress–strain curves of NC gels in the as-prepared state. Samples were compressed to a strain of 90%. (b) Tensile stress–strain curves of NC gels in the as-prepared state.

gels. The curves show that the compressive stress increased with increasing Laponite content because Laponite can tune the mechanical strength of the NC gels by controlling the cross-link

**Figure 6.** Compressive and tensile properties of NC gels. (a–c) Optical images showing that the NC gel samples were very elastic to sustain a high strain compression. (d–g) Optical images showing the process of the NC gels being stretched in a tensile machine. (h) Knotting state.

density of the network structure. In addition, an increase in gelatin content also improved the compressive stress, because gelatin can interpenetrate in the PAAm/Laponite network. As the stresses of L2G2 (208.4 ± 5.9 kPa) and L2G1 (193.2 ± 6.9 kPa) were much higher than that of L2G0 (161.4 ± 5.2 kPa), we conjecture that the gelatin chains not only generate physical entanglements in the hydrogels but also bind to the negatively charged clay through noncovalent interactions such as electrostatic interactions and hydrogen bonds. We also noticed that the LOG2 samples, which were organic hydrogels because of the absence of Laponite, could sustain a high compression during the mechanical test. This is likely because the amount of BIS used in LOG2 was much less than the amount used in conventional organic hydrogels and the interpenetrating gelatin chains in the PAAm network enhanced the mechanical strength of the LOG2 gels.

Figure 7b shows the tensile stress–strain curves of the NC gels in the as-prepared state. For clear comparison, the elongation at break, tensile strength at break, and Young's modulus are also reported in Table 2. The results indicate that

Table 2. Mechanical Properties of NC Gels in the As-Prepared State

sample	Young's modulus (E , kPa)	tensile strength at break (σ_b , kPa)	elongation at break (ϵ_b , %)	compression stress (σ , kPa)
LOG2	7.7 ± 0.1	63.5 ± 1.1	353.1 ± 10.7	89.1 ± 3.8
L1G2	11.4 ± 0.1	159.5 ± 3.5	596.7 ± 26.3	120.3 ± 2.4
L2G2	20.5 ± 0.2	337.9 ± 4.9	750.4 ± 14.7	208.4 ± 5.9
L2G1	14.4 ± 0.1	279.3 ± 7.2	720.8 ± 10.9	193.2 ± 6.9
L2G0	10.6 ± 0.2	262.1 ± 5.6	707.2 ± 15.4	161.4 ± 5.2

the elongation at break of the NC gels was highly dependent on the Laponite content. Also, the Young's modulus and tensile strength at break increased with increasing Laponite content (samples LOG2, L1G2, and L2G2). An extraordinary elongation ratio at break is a typical mechanical property of nanocomposite hydrogels. In the NC gel networks, PAAm chains are cross-linked by the Laponite platelets through noncovalent interactions. Okay and Oppermann⁴³ proposed that a dynamic adsorption/desorption process might occur, that is, the noncovalent interactions between the PAAm chains and the Laponite platelets can be broken and reconstructed constantly when a load is applied to the NC gels and then released. Thus, the polymer chains would be in a dynamic state of adsorbing onto or desorbing from the surfaces of the Laponite platelets. As expected, a high Laponite content would lead to a gel network with a high cross-link density and thus enhance the Young's modulus and tensile strength. It is interesting to note that the introduction of gelatin (samples LOG2, L1G2, and L2G2) contributed to increases in the Young's modulus and tensile strength, further revealing the enhanced compatibility of the gelatin and the PAAm/Laponite system in the present work. As a result, the prepared NC gels exhibited excellent elastic and stretching properties.

Swelling Behaviors. The swelling behavior of the NC gels was investigated at room temperature in solutions of various pH values ranging from 3 to 12 with the ionic strength fixed at 0.01 M. The effects of pH on the equilibrium swelling ratio of the NC gels with different Laponite/gelatin/PAAm weight ratios are shown in Figure 8a. It can be seen that the L2G0 hydrogel was almost unaffected by changes in the pH of the solution, probably due to the fact that PAAm is a nonionic

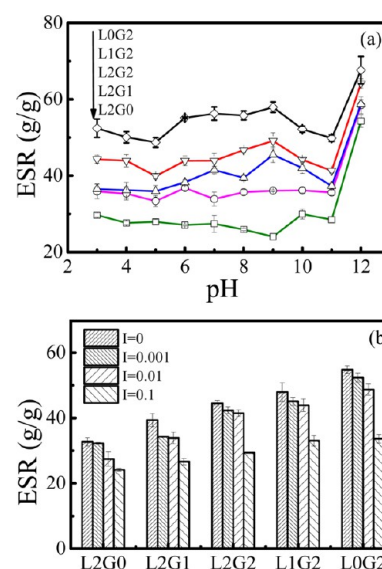


Figure 8. Effects of (a) pH and ionic strength (b) on the equilibrium swelling ratios (ESRs) of the NC gels.

polymer and cannot ionize in aqueous solutions from pH 3 to 11. However, at a pH value of 12, the $-\text{CONH}_2$ groups of PAAm hydrolyzed and induced a considerable increase of the swelling ratio of the network.⁴⁴ The introduction of Laponite seems not lead to any obvious pH-responsive property. However, the samples that contained gelatin all displayed a pH-responsive property giving rise to a W shape in Figure 8a, which is similar to the behavior of pure gelatin in solutions of different pH values.⁴⁵ Therefore, the addition of gelatin to the hydrogels can improve the pH-responsive properties of the NC gels.

The effect of the ionic strength on the equilibrium swelling ratio of the NC gels was investigated and is shown in Figure 8b. The ionic strength of the external solution was varied from 0 to 0.1 M. Figure 8b shows that the equilibrium swelling ratio decreased with increasing ionic strength of the solution. This behavior can be attributed to the reduction in the osmotic pressure difference between the hydrogels and the external solution with increasing ionic strength.⁴⁶ Note that the NC gels with higher gelatin contents and lower Laponite contents were more sensitive to the increase in ionic strength. This is related to the ampholytic polyelectrolyte nature of gelatin because an increase in ionic strength would reduce the electrostatic repulsion between ionized groups such as $-\text{NH}_3^+$ and $-\text{COO}^-$ and induce the shrinkage of the hydrogels. Moreover, a lower Laponite content means a less cross-linked network structure and more free space available for shrinking in the resulting NC gels.

In Vitro Blood Compatibility. Platelets tend to adsorb onto the surface of foreign materials and become activated when biomaterials are used as blood-contacting devices. The activated platelets can further initiate thrombosis by secreting prothrombotic factor, which, in turn, leads to clotting.¹¹ Thrombosis and complement activation are good for hemostatic materials because they can prevent blood loss. However, they are harmful for blood-contacting devices because of the generation of blood clots. Therefore, the biocompatibility of blood-contacting devices is an important issue for different practical applications.⁴⁷ We therefore evaluated the in vitro blood compatibility of the synthesized

gelatin/PAAm/Laponite NC gels based on the amount of protein (BSA) adsorbed, the blood-clotting index, and the degree of hemolysis.

Protein (BSA) adsorption is a critical index for evaluating the blood compatibility of biomaterials because it determines the mechanism and degree of intrinsic thrombosis.⁸ It is well-known that protein adsorption is the first step involved in the initiation of thrombosis on biomaterial surfaces, and thus decreasing BSA adsorption clearly implies a better antithrombotic effect, which can further be confirmed by higher values of blood-clotting index and lower degrees of hemolysis.⁴⁸ Figure 9

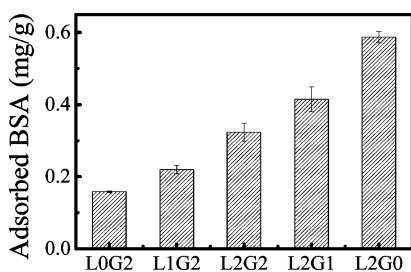


Figure 9. Amounts of BSA adsorbed by gelatin/PAAm/Laponite NC gels. Lower amounts of BSA adsorbed mean better antithrombogenicity of the material.

shows that the amount of BSA adsorbed decreased with increasing gelatin content in the NC gels. This is because gelatin is a hydrophilic and biocompatible polymer in nature, which confers an increased hydrophilicity and wettability on the NC gels and a resulting BSA adsorption resistance. Indeed, it has been reported that a more hydrophilic surface results in a more antithrombotic effect.^{47,49} Obviously, the introduction of gelatin into the NC gels enhanced the blood compatibility of these biomaterials.

The blood-clotting behaviors of the prepared NC hydrogels are shown in Figure 10. Note that a higher blood-clotting index

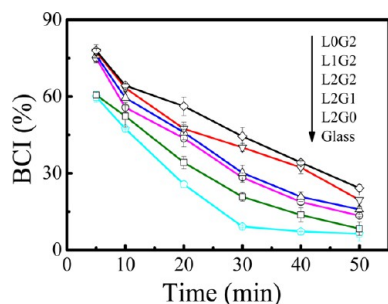


Figure 10. Blood-clotting indexes of the gelatin/PAAm/Laponite NC gels and glass at 37 °C. A higher BCI means a longer clotting time and a better antithrombogenicity.

generally indicates a longer clotting time and a better antithrombotic effect. Compared to glass, all of the hydrogels had higher BCIs, suggesting an improved performance with increasing gelatin content and decreasing Laponite content. These results confirmed those of our previous BSA adsorption test. As a hemocompatible biopolymer, gelatin has been used as plasma expander and blood substitute since the 1940s.^{23,24} In many reported studies, gelatin was found to be able to resist platelet adhesion and thrombin generation by impairing the functionality of the plasma von Willebrand factor (vWF).⁵⁰ Our results also confirm that higher gelatin contents can improve

antithrombogenicity. It has been suggested that a negatively charged surface would initiate the intrinsic pathway of thrombosis by contact activation of factor XII,¹¹ which finally results in the formation of a blood clot. Laponite is a type of nanoclay with a negatively charged surface. Considering the possible applications of NC gels in the biomedical field, we used Laponite contents up to 2% w/v in this study, lower than those in typically reported Laponite NC gels (~5% w/v).⁷

The hemolytic potential of the NC gels was also evaluated based on the degree of erythrolysis and hemoglobin dissociation when the materials were in contact with blood.⁵¹ Figure 11 shows the hemolytic ratios of blood in contact with

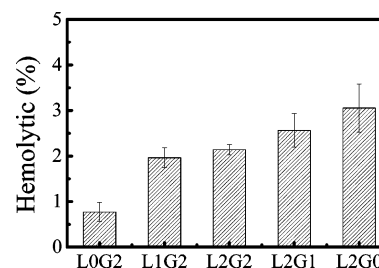


Figure 11. Hemolytic extents of the gelatin/PAAm/Laponite nanocomposite hydrogels at 37 °C for 60 min. The hemolytic extents of all samples were below the permissible level of 5%.

different samples at 37 °C for 60 min. The degrees of hemolysis of all of the samples were below the national and international permissible level of 5%, indicating that all of the hydrogels were nonhemolytic. The hemolytic tests exhibited a trend related to the effects of gelatin and Laponite similar to that observed in the dynamic clotting tests. Our results show that the appropriate ratio of gelatin and Laponite would provide not only improved physicochemical properties to the NC gels but also enhanced blood compatibility.

CONCLUSIONS

In this article, we have reported the successful incorporation of gelatin into the PAAm/Laponite system to prepare a novel hemocompatible gelatin/PAAm/Laponite nanocomposite hydrogel by in situ free-radical polymerization. Our results show that conducting the polymerization at 50 °C and adding AAm and a small amount of BIS can greatly improve the stability and compatibility of the Laponite/gelatin mixture. After the polymerization, both gelatin and PAAm chains were distributed homogeneously in the NC gels. Importantly, the introduction of gelatin did not reduce the transparency of the resultant hydrogels, presumably because the gelatin chains were immobilized in the gel network by noncovalent interactions, such as electrostatic interactions, hydrogen bonds, and physical entanglements. The resultant NC gels were found to be porous materials whose pore size could be tuned by the contents of both gelatin and clay. The hydrogels exhibited good thermal stability and excellent tensile and stretching properties. The addition of gelatin to the hydrogels not only improved the pH-responsive properties but also enhanced the antithrombogenicity of the NC gels. Furthermore, the hemolysis tests revealed that gelatin can decrease the extent of hemolysis and that all of the hydrogels are nonhemolytic. The prepared hydrogels thus have potential in tissue engineering applications as novel porous, hemocompatible, pH-sensitive, and elastic hydrogels.

AUTHOR INFORMATION

Corresponding Authors

*E-mail: wlin@scu.edu.cn (W.L.).

*E-mail: tongai@cuhk.edu.hk (T.N.).

Notes

The authors declare no competing financial interest.

ACKNOWLEDGMENTS

Financial support from the National Natural Science Foundation (NNSF) of China (21176159, 21476148) and the National High-Tech Research and Development Program (863 program) of China (2013AA06A306) is gratefully acknowledged. T.N. acknowledges support from the Hong Kong Special Administration Region (HKSAR) General Research Fund (CUHK402712, 2130304).

REFERENCES

- (1) Zhang, W.; Liu, Y.; Zhu, M.; Zhang, Y.; Liu, X.; Yu, H.; Jiang, Y.; Chen, Y.; Kuckling, D.; Adler, H.-J. P. Surprising Conversion of Nanocomposite Hydrogels with High Mechanical Strength by Posttreatment: From a Low Swelling Ratio to an Ultrahigh Swelling Ratio. *J. Polym. Sci., Part A: Polym. Chem.* **2006**, *44*, 6640–6645.
- (2) Haraguchi, K.; Takehisa, T.; Fan, S. Effects of Clay Content on the Properties of Nanocomposite Hydrogels Composed of Poly(N-isopropylacrylamide) and Clay. *Macromolecules* **2002**, *35*, 10162–10171.
- (3) Haraguchi, K. Nanocomposite Hydrogels. *Curr. Opin. Solid State Mater. Sci.* **2007**, *11*, 47–54.
- (4) Kallukalam, B. C.; Jayabalan, M.; Sankar, V. Studies on Chemically Crosslinkable Carboxy Terminated-poly(propylene fumarate-co-ethylene glycol)-acrylamide Hydrogel as an Injectable Biomaterial. *Biomed. Mater.* **2009**, *4*, 015002.
- (5) Niu, G.; Yang, Y.; Zhang, H.; Yang, J.; Song, L.; Kashima, M.; Yang, Z.; Cao, H.; Zheng, Y.; Zhu, S.; Yang, H. Synthesis and Characterization of Acrylamide/N-vinylpyrrolidone Copolymer with Pendant Thiol Groups for Ophthalmic Applications. *Acta Biomater.* **2009**, *5*, 1056–1063.
- (6) Xiao, J.; Tolbert, T. J. Synthesis of Polymerizable Protein Monomers for Protein-Acrylamide Hydrogel Formation. *Biomacromolecules* **2009**, *10*, 1939–1946.
- (7) Haraguchi, K.; Takehisa, T.; Ebato, M. Control of Cell Cultivation and Cell Sheet Detachment on the Surface of Polymer/Clay Nanocomposite Hydrogels. *Biomacromolecules* **2006**, *7*, 3267–3275.
- (8) Bajpai, A.; Sharma, M. Preparation and Characterization of Novel pH-sensitive Binary Grafted Polymeric Blends of Gelatin and Poly(vinyl alcohol): Water Sorption and Blood Compatibility Study. *J. Appl. Polym. Sci.* **2006**, *100*, 599–617.
- (9) Zhang, M.; Ferrari, M. Hemocompatible Polyethylene Glycol Films on Silicon. *Biomed. Microdevices* **1998**, *1*, 81–89.
- (10) Chang, Y.; Shih, Y.; Ko, C.; Jhong, J.; Liu, Y.; Wei, T. Hemocompatibility of Poly(vinylidene fluoride) Membrane Grafted with Network-like and Brush-like Antifouling Layer Controlled via Plasma-induced Surface PEGylation. *Langmuir* **2011**, *27*, 5445–5455.
- (11) Gorbet, M. B.; Sefton, M. V. Biomaterial-associated Thrombosis: Roles of Coagulation Factors, Complement, Platelets and Leukocytes. *Biomaterials* **2004**, *25*, S681–S703.
- (12) Wendel, H. P.; Ziemer, G. Coating-techniques to Improve the Hemocompatibility of Artificial Devices Used for Extracorporeal Circulation. *Eur. J. Cardio-thorac Surg.* **1999**, *16*, 342–350.
- (13) Redmond, J. M.; Gillinov, A. M.; Stuart, R. S.; Zehr, K. J.; Winkelstein, J. A.; Herskowitz, A.; Cameron, D. E.; Baumgartner, W. A. Heparin-coated Bypass Circuits Reduce Pulmonary Injury. *Ann. Thorac. Surg.* **1993**, *56*, 474–479.
- (14) Gu, Y.; van Oeveren, W.; Akkerman, C.; Boonstra, P. W.; Huyzen, R. J.; Wildevuur, C. R. Heparin-coated Circuits Reduce the

Inflammatory Response to Cardiopulmonary Bypass. *Ann. Thorac. Surg.* **1993**, *55*, 917–922.

(15) Kang, H. W.; Tabata, Y.; Ikada, Y. Fabrication of Porous Gelatin Scaffolds for Tissue Engineering. *Biomaterials* **1999**, *20*, 1339–1344.

(16) Liu, Y.; Chan-Park, M. B. Hydrogel Based on Interpenetrating Polymer Networks of Dextran and Gelatin for Vascular Tissue Engineering. *Biomaterials* **2009**, *30*, 196–207.

(17) Kim, H. W.; Kim, H. E.; Salih, V. Stimulation of Osteoblast Responses to Biomimetic Nanocomposites of Gelatin-Hydroxyapatite for Tissue Engineering Scaffolds. *Biomaterials* **2005**, *26*, 5221–5230.

(18) Balakrishnan, B.; Mohanty, M.; Umashankar, P.; Jayakrishnan, A. Evaluation of an in situ Forming Hydrogel Wound Dressing Based on Oxidized Alginate and Gelatin. *Biomaterials* **2005**, *26*, 6335–6342.

(19) Chang, W. H.; Chang, Y.; Lai, P. H.; Sung, H. W. A Genipin-crosslinked Gelatin Membrane as Wound-dressing Material: in vitro and in vivo Studies. *J. Biomater. Sci., Polym. Ed.* **2003**, *14*, 481–495.

(20) Wang, T.; Zhu, X. K.; Xue, X. T.; Wu, D. Y. Hydrogel Sheets of Chitosan, Honey and Gelatin as Burn Wound Dressings. *Carbohydr. Polym.* **2012**, *88*, 75–83.

(21) Young, S.; Wong, M.; Tabata, Y.; Mikos, A. G. Gelatin as a Delivery Vehicle for the Controlled Release of Bioactive Molecules. *J. Controlled Release* **2005**, *109*, 256–274.

(22) Hamidi, M.; Azadi, A.; Rafiei, P. Hydrogel Nanoparticles in Drug Delivery. *Adv. Drug Delivery Rev.* **2008**, *60*, 1638–1649.

(23) Waters, E. T. A Comparison of Isinglass and Gelatin as Blood Substitutes. *Can. Med. Assoc. J.* **1941**, *45*, 395–398.

(24) Parkins, W.; Koop, C.; Riegel, C.; Vars, H.; Lockwood, J. Gelatin as a Plasma Substitute with Particular Reference to Experimental Hemorrhage and Burn Shock. *Ann. Surg.* **1943**, *118*, 193–214.

(25) Manju, S.; Muraleedharan, C. V.; Rajeev, A.; Jayakrishnan, A.; Joseph, R. Evaluation of Alginate Dialdehyde Cross-linked Gelatin Hydrogel as a Biodegradable Sealant for Polyester Vascular Graft. *J. Biomed. Mater. Res., Part B* **2011**, *98*, 139–149.

(26) Bundela, H.; Bajpai, A. Designing of Hydroxyapatite-Gelatin Based Porous Matrix as Bone Substitute: Correlation with Biocompatibility Aspects. *eXPRESS Polym. Lett.* **2008**, *2*, 201–213.

(27) Schreiber, A. B.; Haimovich, J. Quantitative Fluorometric Assay for Detection and Characterization of Fc Receptors. *Methods Enzymol.* **1983**, *93*, 147–155.

(28) Jain, S.; Bajpai, A. Designing Polyethylene Glycol (PEG)-plasticized Membranes of Poly(vinyl alcohol-g-methyl methacrylate) and Investigation of Water Sorption and Blood Compatibility Behaviors. *Des. Monomers Polym.* **2013**, *16*, 436–446.

(29) Meng, Z. X.; Zheng, W.; Li, L.; Zheng, Y. F. Fabrication and Characterization of Three-dimensional Nanofiber Membrane of PCL-MWCNTs by Electrospinning. *Mater. Sci. Eng., C* **2010**, *30*, 1014–1021.

(30) Cui, L.; Tang, C.; Yin, C. Effects of Quaternization and PEGylation on the Biocompatibility, Enzymatic Degradability and Antioxidant Activity of Chitosan Derivatives. *Carbohydr. Polym.* **2012**, *87*, 2505–2511.

(31) Dawlee, S.; Sugandhi, A.; Balakrishnan, B.; Labarre, D.; Jayakrishnan, A. Oxidized Chondroitin Sulfate-cross-linked Gelatin Matrixes: a New Class of Hydrogels. *Biomacromolecules* **2005**, *6*, 2040–2048.

(32) Pawar, N.; Bohidar, H. B. Spinodal Decomposition and Phase Separation Kinetics in Nanoclay-Biopolymer Solutions. *J. Polym. Sci., Part B: Polym. Phys.* **2010**, *48*, 555–565.

(33) Hu, X.; Xiong, L.; Wang, T.; Lin, Z.; Liu, X.; Tong, Z. Synthesis and Dual Response of Ionic Nanocomposite Hydrogels with Ultrahigh Tensibility and Transparency. *Polymer* **2009**, *50*, 1933–1938.

(34) Xiong, L.; Zhu, M.; Hu, X.; Liu, X.; Tong, Z. Ultrahigh Deformability and Transparency of Hectorite Clay Nanocomposite Hydrogels with Nimble pH Response. *Macromolecules* **2009**, *42*, 3811–3817.

(35) Hou, Y.; Matthews, A. R.; Smitherman, A. M.; Bulick, A. S.; Hahn, M. S.; Hou, H.; Han, A.; Grunlan, M. A. Thermoresponsive Nanocomposite Hydrogels with Cell-releasing Behavior. *Biomaterials* **2008**, *29*, 3175–3184.

(36) Jaiswal, M.; Koul, V.; Dinda, A. K.; Mohanty, S.; Jain, K. G. Cell Adhesion and Proliferation Studies on Semi-interpenetrating Polymeric Networks (semi-IPNs) of Polyacrylamide and Gelatin. *J. Biomed. Mater. Res., Part B* **2011**, *98*, 342–350.

(37) Bajpai, A.; Sharma, M. Preparation and Characterization of Binary Grafted Polymeric Blends of Polyvinyl Alcohol and Gelatin and Evaluation of Their Water Uptake Potential. *J. Macromol. Sci., Part A: Pure Appl. Chem.* **2005**, *42*, 663–682.

(38) Ma, J.; Zhang, L.; Fan, B.; Xu, Y.; Liang, B. A Novel Sodium Carboxymethylcellulose/poly(N-isopropylacrylamide)/Clay Semi-IPN Nanocomposite Hydrogel with Improved Response Rate and Mechanical Properties. *J. Polym. Sci., Part B: Polym. Phys.* **2008**, *46*, 1546–1555.

(39) Sun, J. Y.; Zhao, X.; Illeperuma, W. R.; Chaudhuri, O.; Oh, K. H.; Mooney, D. J.; Vlassak, J. J.; Suo, Z. Highly Stretchable and Tough Hydrogels. *Nature* **2012**, *489*, 133–136.

(40) Zhou, C.; Wu, Q. A Novel Polyacrylamide Nanocomposite Hydrogel Reinforced with Natural Chitosan Nanofibers. *Colloids Surf., B* **2011**, *84*, 155–162.

(41) Jaiswal, M.; Dinda, A. K.; Gupta, A.; Koul, V. Polycaprolactone Diacrylate Crosslinked Biodegradable Semi-interpenetrating Networks of Polyacrylamide and Gelatin for Controlled Drug Delivery. *Biomed. Mater.* **2010**, *5*, 065014.

(42) Karimi, F.; Taheri Qazvini, N.; Namivandi-Zangeneh, R. Fish Gelatin/Laponite Biohybrid Elastic Coacervates: A Complexation Kinetics–Structure Relationship Study. *Int. J. Biol. Macromol.* **2013**, *61*, 102–113.

(43) Okay, O.; Oppermann, W. Polyacrylamide–Clay Nanocomposite Hydrogels: Rheological and Light Scattering Characterization. *Macromolecules* **2007**, *40*, 3378–3387.

(44) Wang, T.; Liu, D.; Lian, C.; Zheng, S.; Liu, X.; Wang, C.; Tong, Z. Rapid Cell Sheet Detachment from Alginate Semi-interpenetrating Nanocomposite Hydrogels of PNIPAm and Hectorite Clay. *React. Funct. Polym.* **2011**, *71*, 447–454.

(45) Gustavson, K. H., Ed. *The Chemistry and Reactivity of Collagen*; Academic Press Inc.: New York, 1956.

(46) Raafat, A. I. Gelatin Based pH-sensitive Hydrogels for Colon-specific Oral Drug Delivery: Synthesis, Characterization, and in vitro Release Study. *J. Appl. Polym. Sci.* **2010**, *118*, 2642–2649.

(47) Menzies, K. L.; Jones, L. The Impact of Contact Angle on the Biocompatibility of Biomaterials. *Optometry Vision Sci.* **2010**, *87*, 387–399.

(48) Shankaraman, V.; Davis-Gorman, G.; Copeland, J. G.; Caplan, M. R.; McDonagh, P. F. Standardized Methods to Quantify Thrombogenicity of Blood-contacting Materials via Thromboelastography. *J. Biomed. Mater. Res., Part B* **2012**, *100*, 230–238.

(49) Kataoka, K.; Ito, H.; Amano, H.; Nagasaki, Y.; Kato, M.; Tsuruta, T.; Suzuki, K.; Okano, T.; Sakurai, Y. Minimized Platelet Interaction with Poly (2-hydroxyethyl methacrylate-block-4-bis(trimethylsilyl) methylstyrene) Hydrogel Showing Anomalously High Free Water Content. *J. Biomater. Sci., Polym. Ed.* **1998**, *9*, 111–129.

(50) Tabuchi, N.; de Haan, J.; Gallandat Huet, R. C.; Boonstra, P. W.; van Oeveren, W. Gelatin Use Impairs Platelet Adhesion During Cardiac Surgery. *Thromb. Haemost.* **1995**, *74*, 1447–1451.

(51) Xiao, K.; Li, Y.; Luo, J.; Lee, J. S.; Xiao, W.; Gonik, A. M.; Agarwal, R. G.; Lam, K. S. The Effect of Surface Charge on in vivo Biodistribution of PEG-oligocholic Acid Based Micellar Nanoparticles. *Biomaterials* **2011**, *32*, 3435–3446.